Supplementary Note 1: classical characterisation of the DOF

Supplementary Figure 1(a) shows a 2D plot of the gain spectrum at the output of the dispersion-oscillating fibre (DOF) for different average $<\beta_2>$ values, which can be chosen by tuning the pump wavelength. While the GVD is positive all along the fiber length, a set of symmetric side bands appears on both sides of the central frequency due to the periodic modulation of the dispersion. The asymmetry in power between the Stokes and anti-Stokes side of the spectrum is due to the contribution of the Raman effect. The position of these parametric sidebands can be accurately predicted from a quasi-phase-matching (QPM) relation [1, 2] (Supplementary References). In order to derive this equation, we recall that in uniform fibers, modulation instability is ruled by a momentum conservation relation. This leads to the following phase matching relation:

$$\beta_2 \Delta\omega^2 + \frac{\beta_4}{12}\Delta\omega^4 + 2\gamma P_p = 0,$$

where $\beta_{2,4}$ is the second and fourth order dispersion terms, γ the nonlinear coefficient, P_p the pump power, and $\Delta\omega$ the frequency shift. By periodically modulating the fiber dispersion over the propagation axis, a dispersion grating must be accounted for in the momentum conservation relation. A significant amplification of unstable frequencies can be achieved in these periodically modulated media if the phase accumulated over one period of modulation is a 2π multiple. It reads as:

$$\int_z^{z+\Lambda} \beta_2(z)\Delta\omega^2 dz + \int_z^{z+\Lambda} \frac{\beta_4(z)}{12} dz \Delta\omega^4 + \int_z^{z+\Lambda} 2\gamma P_p dz = 2m\pi$$

where m is a positive or negative integer, Λ the modulation period. Finally, this leads to:

$$<\beta_2> \Delta\omega^2 + \frac{<\beta_4>}{12}\Delta\omega^4 + 2\gamma P_p = 2m\pi/\Lambda, \quad \text{(S1)}$$

where $<\beta_{2,4}>$ are the average values of the second and fourth order dispersion. This is identical to Eq. (2) in the main text, except for the term with the power dependence, which is completely negligible for $P_p < 1W$. Therefore we have shown that the prediction for DCE represents the low power limit of the QPM relation.

Red dotted lines in Supplementary Figure 1(b) represent the solutions of this equation for $m = 0$ to 4, whereas the colour map of the gain is derived numerically by using the segmentation method described in Ref. [1]. It allows to calculate the amplification gain, including losses, Raman effect and it is faster that a numerical integration of the nonlinear Shrodinger equation. The order $m = 0$ corresponds to the case of a uniform fiber. As evident from the figure this case has no appreciable gain compared to other modes originating from the periodic modulation of the dispersion. QPM curves predict the positions of unstable bands but no information is provided on the gain of these bands. For instance, for an average dispersion value $<\beta_2>= 0.45$ ps^{2}km^{-1} (horizontal dashed line), Eq. (S1) predicts that 9 frequencies can be destabilized (from m=0 to 4), but actually a significant gain exists only for m=1 and m=3 sidebands, as illustrated in Supplementary Figure 1(a) and 1(b). Supplementary Figure 1(b) shows the spectra for $\lambda_p = 1052.44$ nm. The position of the gain bands is in very good agreement with QPM theoretical predictions (black dashed lines) and the overall shape of the spectrum very close to the one given by integrating the nonlinear Schrodinger

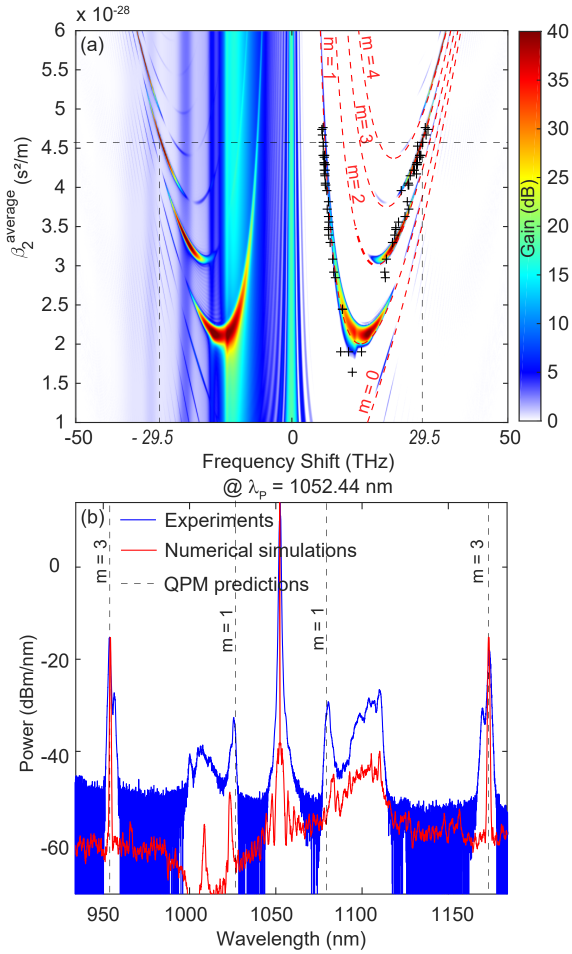

Supplementary Figure 1. **Classical characterization of the fibre.** (a) 2D plot of the parametric gain as a function of the average GVD value calculated from the segmentation method described in Ref. [1]. Red dashed lines correspond to solutions of the QPM relation (Eq.(S1)) for m=0 to 4 and black crosses to experimental measurements for $P_p = 12$ W. (b) Output spectrum, experiments (solid blue line) and numerical simulations (solid red lines) from the nonlinear Schrodinger equation for $<\beta_2>= 0.45$ ps^{2}km^{-1}. Dashed lines represent QPM predictions (Eq.(S1)).

Equation (red line) [3](Supplementary References).

Supplementary Note 2: derivation of Eq. (2) of the main text

Two photons (signal and idler) are excited from the vacuum state by temporal modulation in the comoving frame. As discussed in the main text, in this frame these photons must fulfill the energy conservation condition predicted by the DCE theory:

$$\omega'_s + \omega'_i = m\Omega' + 2\omega'_0.$$

Let us now perform a relativistic boost back into the lab frame by $\omega' = \gamma(\omega - v_g k)$, where $k = k(\omega)$ given by the dispersion relation for the fiber. This yields

$$\gamma(\omega_s - v_g k_s) + \gamma(\omega_i - v_g k_i) = m\gamma(-v_g K) + 2\gamma(\omega_0 - v_g k_0),$$

where we used the fact that the temporal modulation is zero in the lab frame ($\Omega = 0$) and $K = 2\pi/\Lambda$. We can rearrange, and divide by γ, leading to

$$\omega_s + \omega_i - 2\omega_0 = v_g(k_s + k_i - 2k_0) - m v_g K. \tag{S2}$$

Now suppose that $\omega_s = \omega_0 + \Delta\omega$ and $\omega_i = \omega_0 - \Delta\omega$ and expanding k_s and k_i around ω_0:

$$k_s \equiv k(\omega_s) = k(\omega_0 + \Delta\omega) \simeq k_0 + \beta_1 \Delta\omega + \frac{1}{2!}\beta_2 \Delta\omega^2 + \frac{1}{3!}\beta_3 \Delta\omega^3 + \frac{1}{4!}\beta_4 \Delta\omega^4$$

$$k_i \equiv k(\omega_i) = k(\omega_0 - \Delta\omega) \simeq k_0 - \beta_1 \Delta\omega + \frac{1}{2!}\beta_2 \Delta\omega^2 - \frac{1}{3!}\beta_3 \Delta\omega^3 + \frac{1}{4!}\beta_4 \Delta\omega^4$$

If we substitute these into Eq. (S2), we find

$$0 = v_g(\beta_2 \Delta\omega^2 + \frac{1}{12}\beta_4 \Delta\omega^4) - m v_g K.$$

Dividing by v_g this yields Eq. (2) of the main text:

$$\beta_2 \Delta\omega^2 + \frac{1}{12}\beta_4 \Delta\omega^4 = mK. \tag{S3}$$

By using the same argument as in the previous section, one can replace $\beta_{2,4}$ with the average values $< \beta_{2,4} >$, yielding an equation which at low powers is identical to the QPM condition Eq. (S1).

Supplementary Note 3: signal and idler spectra at low power

Supplementary Figure 2 illustrates spectra for signal (left panel) and idler (right panel) taken with the setup for quantum correlations described in the main manuscript. The spectra are acquired by scanning the position of the slits after the first grating G1 (resolution of 1 nm) around the position for which the CAR is maximum. The sharp peaks (less than 1 nm FWHM) in both channels correspond to DCE pairs production and they depend quadratically on the pump power, whereas

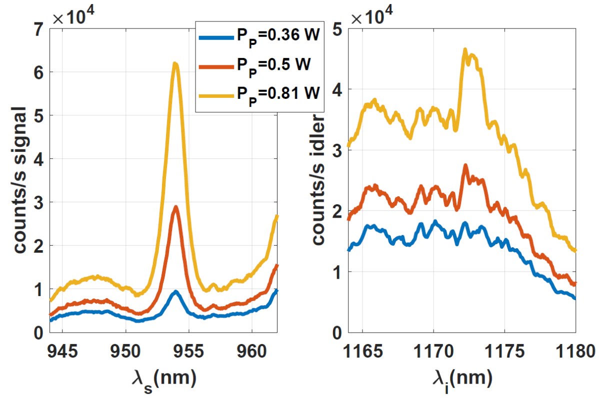

Supplementary Figure 2. **Spectra with single photon detectors.** Spectra of the light measured at low pump power with single photon detectors on the signal (left) and idler (right) channels.

the bulk of the emission on the idler consists of Raman photons, which scale linearly with the pump power. The signal has also a small contribution from Raman which however can be neglected, compared to the DCE contribution.

The ratio between the peaks on signal and idler is assigned to different collection efficiencies of the double grating system for spectral filtering.

SPAD dark counts also contribute to the spectra, but can be neglected in time correlation measurements. Raman photons, on the other hand, cannot be neglected and they will be discussed in the next section. When the pump power is reduced to the levels used in the manuscript for time correlation measurements ($P_p < 0.15$ W), the DCE peaks are no longer distinguishable from the background noise (mainly Raman for idler and dark counts for signal). In the next section we will see how we estimate the DCE pair contribution and separate it from the Raman contribution in quantum correlation measurements (CAR).

Supplementary Note 4: coincidence to accidental ratio (CAR)

The rates of single counts measured on the 3 detectors are called N_{s1} and N_{s2} for the two ports of the beam splitter s1 and s2 on the signal side and N_i for the idler (see setup in Fig. 1(b) of the main text). The count rate on the idler channel is composed of two sources, photons from DCE and photons from Raman scattering of the pump, $N_i = N_{ip} + N_{ir}$, where p stands for pairs and r stands for Raman. $N_{s1} \approx N_{1p}$ and $N_{s2} \approx N_{2p}$, as Raman contribution on the anti-Stokes side of the spectrum is negligible.

The number of coincidences between signal (we will consider s1 from now on, but the same is valid for s2) and idler at zero delay in a Δt time window is called $N_{s,i}(0)$ and it is made of two contributions:

$$N_{s,i}(0) = N^{real}_{s,i} + N^{acc}_{s,i}$$

Let us analyze these two terms:

- *real* (quantum) coincidences $N_{s,i}^{real}$: a single photon from a pair is detected in the signal channel and its twin photon from the same pair is detected in the idler channel. This kind of coincidences takes the form:

$$N_{s,i}^{real} = N_s\eta_i = N_{ip}\eta_1$$

where η_x is the total collection and detection efficiency of channel x. This can be estimated by characterizing the losses of the grating system and the detectors quantum efficiency: $\eta_1 = 2.4\%$, $\eta_2 = 14\%$ and $\eta_i = 1.2\%$. The strong asymmetry between s1 and s2 is assigned to the different quantum efficiency of the detectors (infrared InGaAs single photon detectors on channel s1 and on channel i and a visible Si single photon detector on channel s2). The formula can be derived easily by considering that for each photon of a pair detected on the signal channel there is always a photon on the idler channel with probability 1, however this photon is detected with efficiency η_i, hence the product $N_s\eta_i$.

- *accidental* coincidences $N_{s,i}^{acc}$: given a certain detection time window Δt there is always a probability that a photon, which can be from Raman or from an uncorrelated pair (i.e. from a different temporal mode of the laser), randomly falls within this window. For each photon detected on the signal the probability to have another photon on the idler is simply the number of the total counts detected on the idler divided by the repetition rate of the laser R:

$$N_{s,i}^{acc} = N_s(N_{ip} + N_{ir})/R$$

Photon counts on signal can also be correlated with photon counts on idler delayed by τ where τ corresponds to multiples of the laser pulse periodicity $\pm n/R$ ($n = 1, 2...$). In this case the only possible coincidences consist of accidental ones, so $N_{s,i}(\tau) = N_{s,i}^{acc}(0)$. From this consideration one gets a good approximation of the CAR by using the formula given in the main manuscript:

$$CAR = \frac{N_{s,i}(0) - N_{s,i}(\tau)}{N_{s,i}(\tau)}$$

We use the formulas for real and accidental coincidences in order to model the dependence of the CAR on the pump power (Fig. 4(a) of the manuscript). In this model we have 2 free parameters: the DCE gain (number of pairs per pump pulse per Watt of peak power) and the ratio between Raman N_{ir} and DCE pairs N_{ip} on the idler side. The number of counts from DCE pairs and Raman scattering as a function of the pump power is illustrated in Supplementary Figure 3. At low pump power the measured rates are dominated by the detectors dark counts ($\approx 1000/s$), which makes impossible to estimate

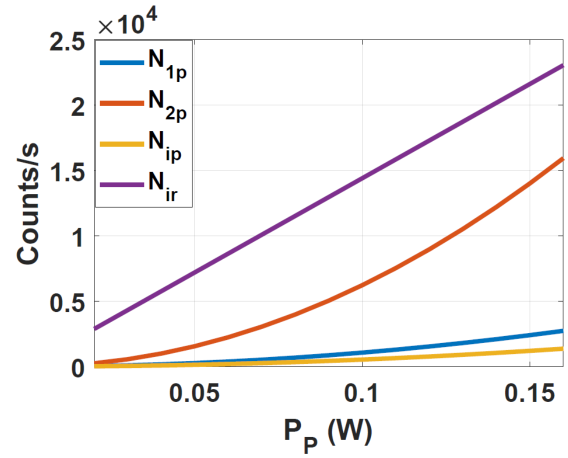

Supplementary Figure 3. **Raman and Casimir photons.** Single counts as a function of the pump peak power P_p for the 3 channels. Only DCE photon rates N_{1p} and N_{2p} are considered on s1 and s2, whereas the rate is broken down between Raman N_{ir} and DCE pairs N_{ip} on the idler channel. The single count rates N_{s1}, N_{s2} and $N_i = N_{ip} + N_{ir}$ at high power ($P_p = 0.15$ W), where the dark counts are negligible, correspond to the measured rates. The rest of the curve is estimated by assuming a linear dependence for Raman and a quadratic dependence for the DCE photons.

N_{s1}, N_{s2} and N_i. However accidental coincidences from dark counts are distributed homogenously at all delays τ, whereas coincidences from Raman and DCE counts bunch around peaks corresponding to the duration and frequency of the pump pulses, making their contribution to CAR completely negligible. We can estimate DCE and Raman rates at low powers by assuming a linear dependence for Raman and a quadratic dependence for the DCE photons. At high power ($P_p = 0.15$ W), where the dark counts are negligible, the single count rates N_{s1}, N_{s2} and N_i in Supplementary Figure 3 correspond to the actually measured rates. Notice that most of the counts on the idler are actually from Raman (compare N_{ir} with N_{ip}), especially at low power, and yet the CAR is still well above 1. From the model we can also estimate that for $P_p = 0.03W$ about 2 10^{-3} DCE pairs are generated by each pump pulse, as opposed to 0.18 Raman photons.

Supplementary Note 5: estimation of the expected $g^{(2)}(0)$

The intensity auto-correlation function $g^{(2)}(0)$ is calculated according to the formula:

$$g^{(2)}(0) = \frac{N_{s1,s2,i}N_i}{N_{s1,i}N_{s2,i}}$$

The double coincidences $N_{s1,i}$ and $N_{s2,i}$ are calculated as described in the previous section. In the simplest case where DCE pairs are made only by single photons all triple coincidences are accidental and they can arise in 2 ways:

- completely accidental triple coincidences of the form: $N_1 \frac{N_2}{R} \frac{N_i}{R}$, where N_i includes both the contribution of Raman and DCE photons
- real coincidences between s1 (or s2) and idler plus an accidental count on s2 (or s1 respectively): $N_1 \eta_i \frac{N_2}{R}$

By considering these contributions and by using the values for N_1, N_2 and N_i estimated in the previous section, we predict the dashed curve presented in Fig. 4(b) of the main text.

[1] Mussot, A., Conforti, M., Trillo, S., Copie, F. & Kudlinski, A. Modulation instability in dispersion oscillating fibers. *Adv. Opt. Photon.* **10**. URL http://aop.osa.org/abstract.cfm?URI=aop-10-1-1.

[2] Droques, M. *et al.* Fourth-order dispersion mediated modulation instability in dispersion oscillating fibers. *Opt. Lett.* **38**. URL http://ol.osa.org/abstract.cfm?URI=ol-38-17-3464.

[3] *Nonlinear Fiber Optics, Fifth Edition* (Academic Press, Amsterdam), 5 edition edn.